OPTIMIZING CODED 16-APSK FOR AERONAUTICAL TELEMETRY

Michael Rice, Chad Josephson
Department of Electrical & Computer Engineering
Brigham Young University
Provo, Utah, USA
mdr@byu.edu, chadcjosephson@gmail.com

Erik Perrins
Electrical Engineering & Computer Science Department
University of Kansas
Lawrence, Kansas, USA
esp@ku.edu

ABSTRACT

This paper investigates the application of 16-APSK modulation to aeronautical mobile telemetry. The peak-to-average power ratio vs. code rate tradeoff is mapped to an optimization problem involving spectral efficiency and the constellation parameters. The optimization results produce a theoretically optimum solution that is 3.95 times more spectrally efficient as uncoded SOQPSK-TG. When implementation losses and the available IRIG 106 LDPC code rates are factored in, the advantage drops to 3.20 times the spectral efficiency of SOQPSK-TG.

INTRODUCTION

In the wake of recent spectral reallocations, such as the AWS-3 auctions that reallocated 1755 – 1780 MHz and 2155–2180 MHz from US Government use to commercial wireless services [1], spectral efficiency in aeronautical mobile telemetry (AMT) has become an even more important topic. One of the efforts to increase spectral efficiency has been an investigation of the application of non-binary linear modulations in the AMT environment. But linear modulations achieve improved spectral efficiency (relative to SOQPSK-TG) at the expense of amplitude variations, quantified by the peak-to-average power ratio (PAPR). Whereas SOQPSK has a PAPR of 0 dB, band-limited linear modulations have a PAPR greater than 0 dB. This necessitates lowering the

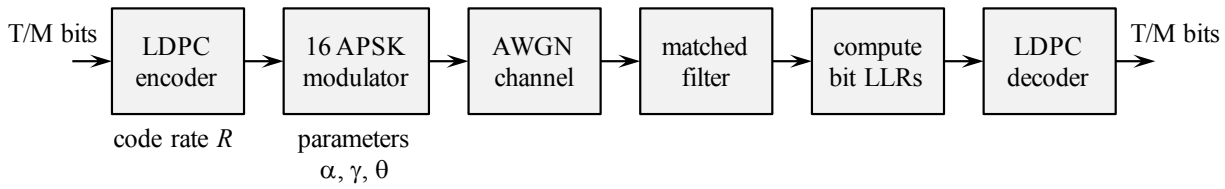

Figure 1: A block diagram an LDPC-coded 16-APSK system for aeronautical telemetry.

operating point of the RF power amplifier to accommodate the amplitude variations without distortion. Lowering the operating point reduces the available transmit power which, in turn, reduces the link margin or transmitter-to-receiver distance. This loss can be recovered using an error correcting code. But error correcting codes increase the bandwidth and therefor reduce the spectral efficiency gains. It might be that the code rate required to compensate for reduced RF power produces a system whose spectral efficiency is not appreciably better than that of uncoded SOQPSK-TG!

Motivated by the good properties of the APSK family of modulations adopted by the digital video broadcast, system 2 (DVB-S2) satellite standard [2], Shaw and Rice [3] explored the use of 16- and 32-APSK with turbo codes in the AMT. The results showed that 16-APSK with rate-$4/5$ turbo codes is able to achieve spectral efficiency approximately 3 times that of uncoded SOQPSK-TG.

Here the performance of 16-APSK with the LDPC codes defined in Appendix R of IRIG 106-15 [4] is explored. The impact of pulse shape and constellation parameters on PAPR is quantified and used to describe the PAPR vs. code rate trade-off. This trade-off is recast to an optimization problem involving spectral efficiency and the constellation parameters. The optimization is used to identify the 16-APSK parameters that maximize the theoretically optimum code. The solution is a set of modulation and code parameters that is 3.95 times more spectrally efficient than uncoded SOQPSK-TG. When implementation losses and the limited IRIG 106 LDPC code rates are factored in, the advantage drops to 3.20 times the spectral efficiency of SOQPSK-TG.

PROBLEM FORMULATION

The block diagram of the system under consideration is shown in Figure 1. Telemetry bits are encoded using an LDPC encoder with rate $0 < R < 1$. The coded bits are used to modulate a carrier using 16-APSK. The complex-valued lowpass equivalent of the 16-APSK modulated carrier is

$$s(t) = \sum_k a_k p(t - kT_s) \tag{1}$$

where $a_k \in \mathcal{C}$ is the k-th symbol which is one of the constellation points in the set $\mathcal{C}$ shown in Figure 2, $p(t)$ is a unit-energy version of the square-root raised-cosine pulse shape [5] with excess bandwidth $0 < \alpha \leq 1$, and T_s is the symbol time.

The received signal is $r(t) = s(t) + w(t)$ where $w(t)$ is the additive thermal noise modeled as

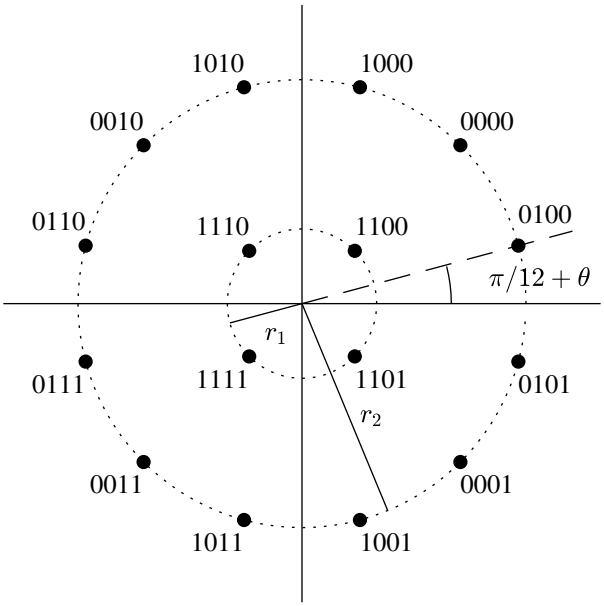

Figure 2: The 16-APSK constellation with the DVB-S2 bit-to-symbol mappings.

a complex-valued normal random process whose in-phase and quadrature components are real-valued wide-sense stationary normal random processes with zero mean and power spectral density N_0 W/Hz [6]. The received signal is matched filtered and sampled at the optimum sampling instants (perfect synchronization is assumed). The log-likelihood ratios (LLRs) are computed for each of the four bits corresponding to each symbol. The log-likelihood ratios form the inputs to the LDPC decoder. The LDPC decoder outputs are estimates of the input bits. The bit error rate is measured by the difference between the bits at the LDPC encoder input and the bits at the LDPC decoder output.

The block diagram shows the four parameters to be optimized in this paper.

MAJOR FACTORS INVOLVED IN THE OPTIMZATION

A. CONSTELLATION PROPERTIES

The 16-APSK constellation shown in Figure 2 comprises four points on a circle of radius r_1 and twelve points on a circle of radius r_2, with $r_2 > r_1$. The points on the outer circle are offset by the angle θ as shown. The constellation is parameterized by $\gamma = r_2/r_1$ and θ. For example, the DVB-S2 standard defines $\gamma = 3.15$, 2.85, 2.75, 2.70, 2.60, and 2.57, all with $\theta = 0$, for $R = {}^{2}/_{3}$, ${}^{3}/_{4}$, ${}^{4}/_{5}$, ${}^{5}/_{6}$, ${}^{8}/_{9}$, and ${}^{9}/_{10}$, respectively, for 16-APSK [2].

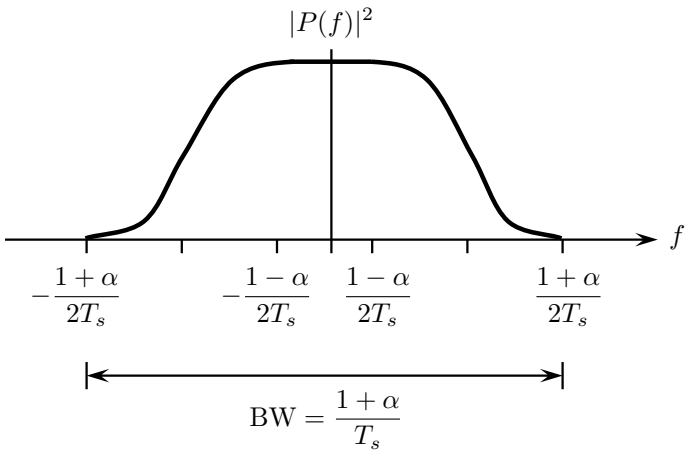

Figure 3: The frequency-domain representation of the SRRC pulse shape.

The average energy of the constellation is

$$E_{\text{avg}} = \frac{1}{16}\sum_{m=0}^{15} |c_m|^2 = \frac{r_1^2 + 3r_2^2}{4} = \frac{1+3\gamma^2}{4} r_1^2, \tag{2}$$

where $c_0, \ldots, c_{15}$ are the 16 complex-valued points in the constellation $\mathcal{C}$.

B. PULSE SHAPE PROPERTIES

The square-root raised-cosine (SRRC) pulse shape ideally provides absolute bandlimiting without producing intersymbol interference [5]. The spectrum of the SRRC pulse shape is illustrated in Figure 3. Observe that the RF bandwidth is defined by the two-sided bandwidth of $|P(f)|^2$ and is parameterized by α, called the "rolloff factor" or "excess bandwidth." The RF bandwidth may be expressed in terms of code rate and the input (information) bit rate:

$$\text{BW} = \frac{1+\alpha}{4R} \times \text{ bit rate.} \tag{3}$$

C. PEAK-TO-AVERAGE POWER RATIO

The power in $s(t)$ given by (1) is proportional to $|s(t)|^2$. The peak power proportional to $\max_t |s(t)|^2$ and the mean (or average) power is $\mathrm{E}\{|s(t)|^2\}$ where the expectation is over both the symbol sequence and time. The peak-to-average power ratio (PAPR) is the ratio of the two:

$$\text{PAPR} = \frac{\max_t |s(t)|^2}{\mathrm{E}\{|s(t)|^2\}}. \tag{4}$$

PAPR is important for RF power amplifier design. RF power amplifier efficiency (measured by ratio of RF output power to DC input power) is maximized when the RF power amplifier oper-

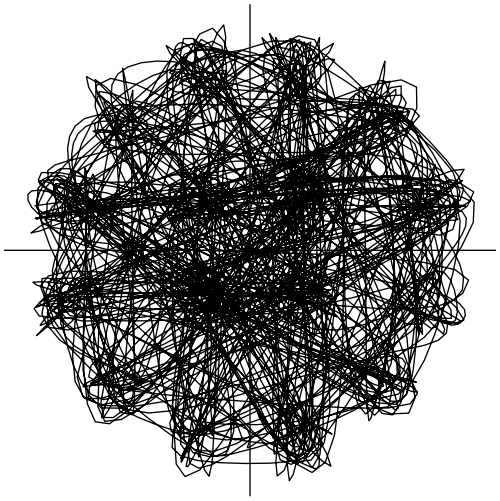

Figure 4: The phase trajectory (quadrature component vs. in-phase component) for 16-APSK ($\gamma = 2.75$, $\theta = 0$) and the SRRC pulse shape with $\alpha = 0.5$.

ates in full saturation. Operating in full saturation imposes amplitude distortion on the transmitted waveform. This distortion causes unwanted sidelobes (called "spectral regrowth") in the spectrum of modulated carriers with amplitude variations. For this reason, waveforms with no amplitude variations, or PAPR = 1 (0 dB), such as PCM/FM, SOQPSK-TG, and ARTM CPM [4] have been preferred in aeronautical telemetry. When a waveform with PAPR > 1 is used, the RF power amplifier must operate in its "linear region" which necessarily reduces both the peak and the average output power. The reduction in average output power is usually called output back-off (OBO). Here, we assume the required OBO is the PAPR. Under this assumption, PAPR is a direct measure of the required OBO.

There are two contributors to PAPR [7]. The first contributor is the arrangement of constellation points. If all the constellation points are on a circle (such as BPSK and QPSK) then the constellation's contribution to the PAPR is zero. Otherwise, the arrangement of points contributes to PAPR. The second contributor is the waveform variation due to the pulse shape. This is illustrated by the phase trajectory (quadrature component vs. in-phase component) of 16-APSK with the SRRC pulse shape with $\alpha = 0.5$ illustrated in Figure 4. The distance from the origin to any point on the phase trajectory represents $|s(t)|$. If $|s(t)|$ were a constant, the phase trajectory would be a circle. Clearly, this is not the case. Note that the peak values of $|s(t)|$ occur in the "overshoot" associated with the constellation points on the outer circle.

The PAPR is a complicated function of the pulse shape parameter α and the constellation parameters γ and θ. We first explore PAPR as a function of α. Figure 5 shows a plot of PAPR for five different 16-ary constellations: the traditional square 16-QAM constellation, the unconstrained optimum (minimum probability of error) constellation, the constrained optimum (minimum probability of error) constellation where the points are constrained to a regular grid, the 16-APSK constellation with $\gamma = 2.75$ and $\theta = 0$, and 16-PSK [5]. To compute the PAPR, a discrete-time version of (1) was generated at a sample rate equivalent to 10 samples/symbol. Because the PAPR

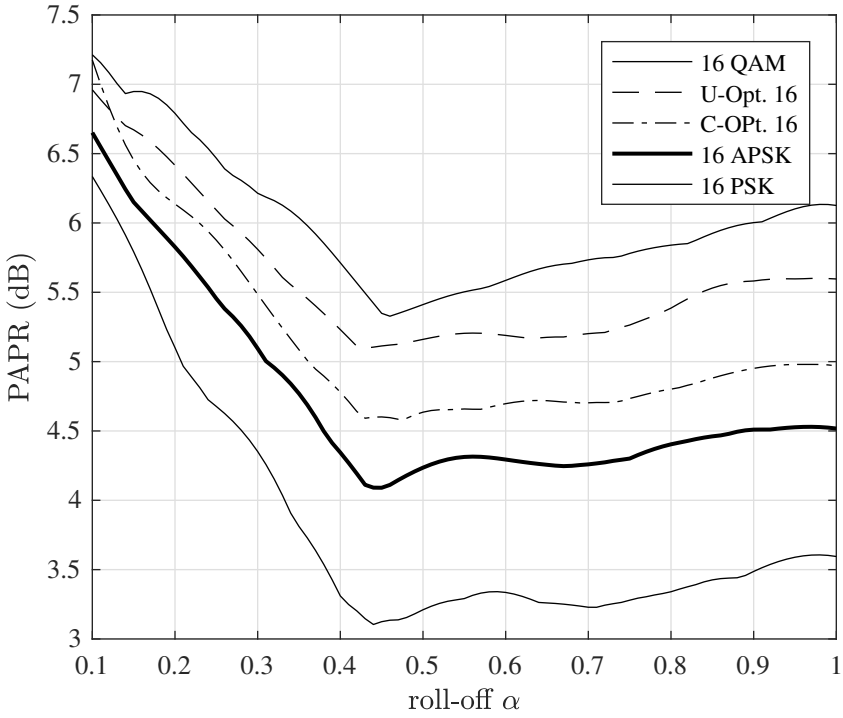

Figure 5: PAPR (dB) vs. SRRC roll-off α for a number of different 16-ary constellations.

depends on the symbol sequence, the symbol sequence corresponding to four repetitions of the length-$32{,}767$ PN sequence (sometimes called the "PN15" sequence because $2^{15} = 32{,}768$) was used as a bit sequence representative of an encrypted telemetry data bit sequence. The results show that the traditional square 16-QAM constellation has the highest PAPR, followed by the unconstrained and constrained optimum constellations. The PAPR of 16-APSK is about 1.5 dB less than that of 16-QAM. Because the 16-PSK constellations positions all the constellation points on a circle, 16-PSK has the lowest PAPR, but it also has the worst bit error probability and therefore requires a lower code rate than the other options.

For all constellations, PAPR is quite high for $\alpha < 0.4$. This demonstrates that even though small α decreases the occupied bandwidth [see Equation (3)], the bandwidth reduction is achieved at the cost of increased PAPR. The optimum (in the sense of minimum PAPR) α is $0.4 < \alpha < 0.5$.

For $\alpha = 0.5$ PAPR for 16-APSK as a function of γ and θ may now be explored. The results are shown in Figure 6. The plot shows that PAPR is a strong function of γ but only weakly dependent on θ.

D. CODE RATE

As explained in the Problem Formulation, a rate-R code, for $0 < R < 1$, produces $1/R$ coded bits for each input (information) bit. If the input (information) bit interval is T_b seconds, then the coded bit interval is $T_c = RT_b$. Because 16-APSK uses four bits per symbol (see the bit-to-symbol labels

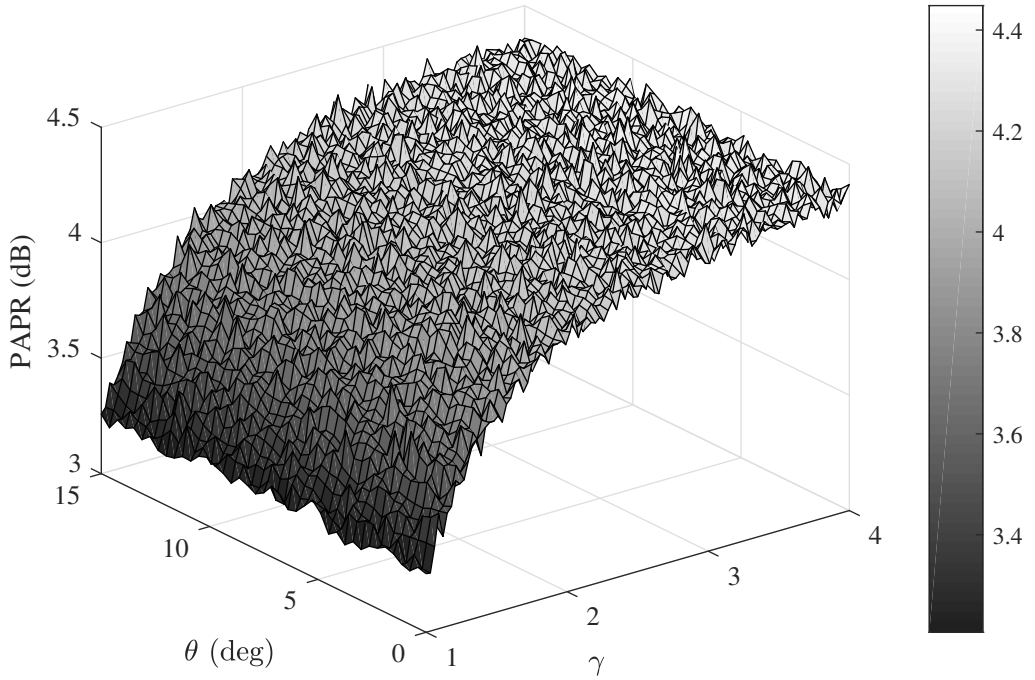

Figure 6: Peak-to-average power ratio (PAPR) for 16-APSK as a function of γ and θ.

in Figure 2), the symbol time in Equation (1) is $T_s = 4T_c$. The resulting bandwidth expansion is inversely proportional to the code rate as indicated in Equation (3).

When attempting to optimize a coded system, the performance of 16-APSK for an arbitrary code rate is of interest. One might envision designing a large number of LDPC codes, each with a different code rate, and simulating the performance of each one for all interesting (γ, θ)-variants of 16-APSK. Unfortunately, the bit error rate performance of coded systems is notoriously difficult to simulate. In light of this difficulty, we resort to concepts from information theory to bound the performance of coded 16-APSK.

Let $x \in \mathcal{C}$ be a constellation point and let $y = x + n$ be the corresponding matched filter output. Given the assumptions for $w(t)$ outlined in the Problem Formulation, n is a complex-valued circularly symmetric normal random variable with zero mean and variance $2\sigma^2$ [i.e., the real part of n (in-phase component) and the imaginary part of n (quadrature component) have the same variance σ^2]. Consequently, y is conditionally normal with density function

$$f(y|x) = \frac{1}{2\pi\sigma^2} \exp\left\{-\frac{1}{2\sigma^2}\left|y - x\right|^2\right\}. \tag{5}$$

For notational purposes below, we write $y = y_R + jy_I$ and $x = a + jb$, and express the conditional density function (5) as the joint density

$$f(y_R, y_I|x) = \frac{1}{2\pi\sigma^2} \exp\left\{-\frac{1}{2\sigma^2}\left[(y_R - a)^2 + (y_I - b)^2\right]\right\}. \tag{6}$$

The symmetric information rate between x and y is the mutual information [8] between x and y

assuming a uniform distribution on x (i.e., the constellation points are equally likely):

$$I(x;y) = \frac{1}{16}\sum_{m=0}^{15}\int_{-\infty}^{\infty}\int_{-\infty}^{\infty} f(y_R, y_I|c_m)\log_2\left\{\frac{f(y_R, y_I|c_m)}{1/16\sum_{m'=0}^{15} f(y_R, y_I|c_{m'})}\right\} dy_R dy_I. \quad (7)$$

The units for $I(x;y)$ are bits/symbol. For example, because 16-APSK uses four bits per symbol, using a rate-$1/2$ code with 16-APSK results in 2 bits/symbol, a rate-$3/4$ code results in 3 bits/symbol, and so on.

The symmetric information rate is an *upper bound* on the number bits/symbol for which it is possible to achieve reliable communications [8]. The corresponding code rate is $I(x;y)/4$. Thus, the interpretation of these results is that is possible to achieve reliable (error-free) bit error rate performance with coded 16-APSK as long as the code rate $R < I(x;y)/4$.

An example illustrates the concept. The symmetric information rate (7) for 16-APSK with $\gamma = 2.75$ and $\theta = 0$ is plotted[1] in Figure 7. $I(x;y) = 1$ bit/symbol at $E_b/N_0 = 0$ dB. This means that reliable communication can be achieved at $E_b/N_0 = 0$ dB using a code with $R < 1/4$. Similarly, $I(x;y) = 2$ bits/symbol at $E_b/N_0 = 2$ dB which means reliable communications can be achieved at $E_b/N_0 = 2$ dB using a code with $R < 1/2$; and $I(x;y) = 3$ bits/symbol at $E_b/N_0 = 4.55$ dB which means reliable communications can be achieved at $E_b/N_0 = 4.55$ dB using a code with $R < 3/4$. Note that as E_b/N_0 increases, the symmetric information rate approaches 4 bits/symbol, which means at these high values of E_b/N_0, a high rate code ($R \to 1$) may be used.

A closely related concept is the maximum code rate for a non-zero probability of error. The relationship between the decoder output bit error probability p, the code rate R and the signal-to-noise ratio is given by [9]

$$R = \frac{I(x;y)}{1 - H_2(p)}, \quad (9)$$

where $H_2(p)$ is the entropy of a binary random variable and is given by [8]

$$H_2(p) = p\log_2(p) + (1-p)\log_2(1-p). \quad (10)$$

For fixed code rate, (9) relates the decoder output probability of error to the signal-to-noise ratio E_b/N_0 for a given constellation. This relationship is plotted in Figure 8 for 16-APSK with $\gamma = 2.75$ and $\theta = 0$ for code rates $1/2$, $2/3$, $3/4$, and $4/5$. (These rates were selected because Appendix R of

[1]Here we have followed the convention of expressing the symmetric information rate in terms of the equivalent uncoded signal-to-noise ratio E_b/N_0. (E_b is the uncoded bit energy and N_0 is the power spectral density of the inphase and quadrature components of the noise.) Because the modulation is 16-APSK, we have $E_{\text{avg}} = 4E_c$, where E_c is the coded-bit energy, and $E_c = RE_b$. Consequently, E_{avg}/N_0 is the over-the-air signal-to-noise ratio at which the synchronizers must operate and E_b/N_0 is the signal-to-noise ratio for the uncoded bits (and without the corresponding bandwidth expansion). The relationship between σ^2 in (7) and the equivalent uncoded signal-to-noise ratio E_b/N_0 is

$$\sigma^2 = \frac{E_{\text{avg}}}{8R\left(\frac{E_b}{N_0}\right)}, \quad (8)$$

where E_{avg} is given by (2) and $R = I(x;y)/4$.

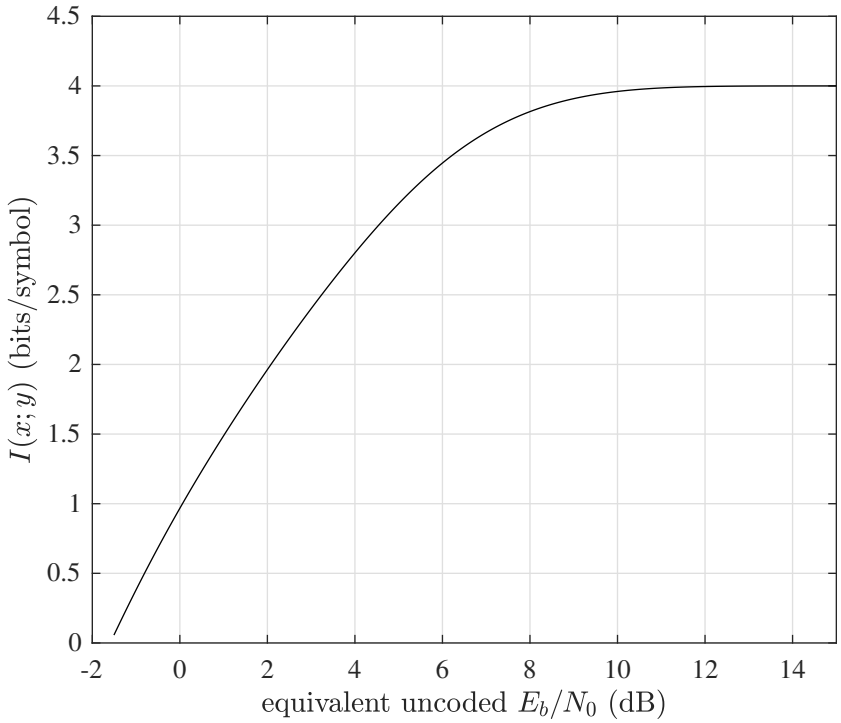

Figure 7: The symmetric information rate (7) vs. E_b/N_0 for 16-APSK with $\gamma = 2.75$ and $\theta = 0$.

IRIG 106-15 [4] defines codes of rates $1/2$, $2/3$, and $4/5$.) The bit error probability vs. E_b/N_0 curve for uncoded SOQPSK-TG is included for reference.

The interpretation is that the code curves define a theoretical boundary. A realizable system must operate to the right of its corresponding curve. For example, when using this version of 16-APSK with a rate-$4/5$ code, the equivalent E_b/N_0 must be greater than 4.55 dB to achieve $p < 10^{-6}$. If $E_b/N_0 > 1.55$ dB cannot be achieved, then either a higher p must be tolerated, or a lower code rate must be used. The bit error probably curve for uncoded SOQPSK-TG, calculated from the analytical expression [10, Equation (15)], is also included for reference. The number of deciBels separating the uncoded SOQPSK-TG curve and one of the code curves upper bounds the coding gain associated with the code and corresponding constellation. It should be pointed out that codes used in practice have coding gains less than those predicted here.

The curves in Figure 8 are consistent with the symmetric information rate of Figure 7. For example, the $R = 1/2$ curve in Figure 8 asymptotically approaches $p = 0$ slightly above $E_b/N_0 = 2$ dB. Because $R = 1/2$ corresponds to $I(x;y) = 2$ bits/symbol, the curve in Figure 7 crosses 2 bits/symbol just above $E_b/N_0 = 2$ dB as well. Similarly, the $R = 3/4$ curve in Figure 8 asymptotically approaches $p = 0$ at $E_b/N_0 = 4.55$ dB and the curve in Figure 7 crosses 3 bits/symbol at the same value of E_b/N_0.

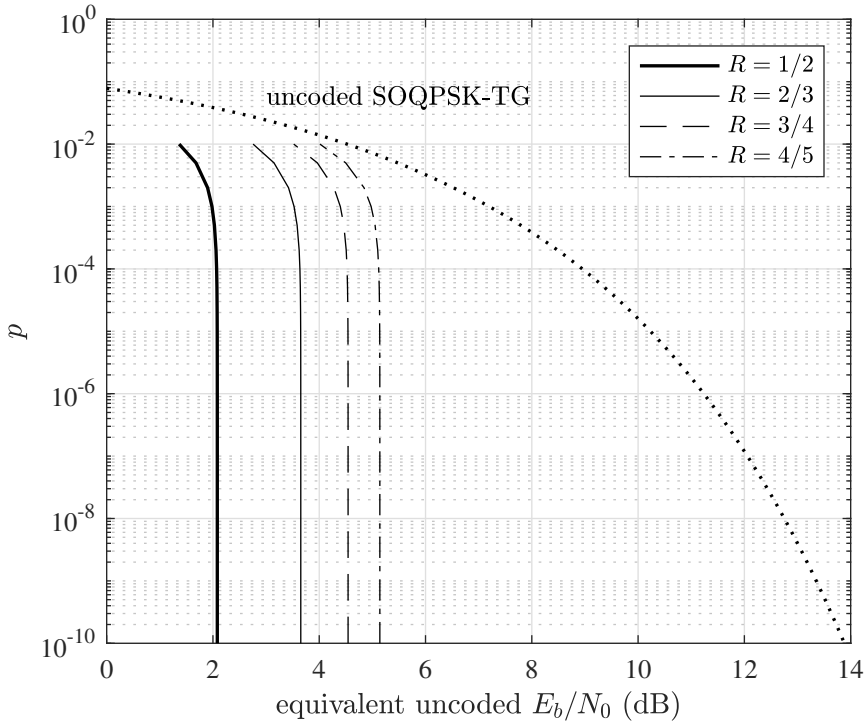

Figure 8: A graphical interpretation of (9): decoder output probability of error vs. signal-to-noise ratio for code rates $1/2$, $2/3$, $3/4$, and $4/5$ for 16-APSK with $\gamma = 2.75$ and $\theta = 0$. The bit error probability curve for SOQPSK-TG is included for reference.

E. SPECTRAL EFFICIENCY

The spectral efficiency of coded 16-APSK is the ratio of (information) bit rate to RF bandwidth and has units bits/s/Hz. The spectral efficiency is [see Equation (3)]

$$\eta = \frac{4R}{1+\alpha} \qquad \text{bits/s/Hz.} \tag{11}$$

The best spectral efficiency is achieved when R is as close to 1 as possible and α is as close to 0 as possible. But these are competing demands. As α decreases, the PAPR increases, which increases the OBO, which, in turn, demands a lower code rate.

OPTIMIZATION

With all the pieces of the previous section now in place, we are in a position to optimize the constellation parameters. The optimization criterion is spectral efficiency (11) which, for fixed α, is proportional to the code rate R. Because the code rate R is proportional to the symmetric information rate $I(x;y)$, maximizing spectral efficiency is the same as maximizing code rate.

The optimization is outlined as follows:

1. Select a reference operating point, $(E_b/N_0)^*$. The operating point is defined by the desired probability of bit error p. The goal is "error-free" performance, which is open to some interpretation. In the example that follows, we choose $p^* = 10^{-10}$ as the definition of "error free" ($p = 10^{-10}$ corresponds to 1 error every 17 minutes for a 10 Mbit/s link or 1 error every 83 minutes for a 2 Mbit/s link). For uncoded SOQPSK-TG, $p = 10^{-10}$ requires (see Figure 8)
$$\left[\left(\frac{E_b}{N_0}\right)^*\right]_{\text{dB}} = 13.9 \text{ dB}. \tag{12}$$

2. The 16-APSK operating point is determined by the OBO, which we equate to the PAPR. Thus, for a given (γ, θ) pair, the corresponding PAPR(γ, θ) defines the 16-APSK operating point as
$$\left[\frac{E_b}{N_0}(\gamma, \theta)\right]_{\text{dB}} = \left[\left(\frac{E_b}{N_0}\right)^*\right]_{\text{dB}} - \left[\text{PAPR}(\gamma, \theta)\right]_{\text{dB}} \tag{13}$$

3. The symmetric information rate corresponding to the 16-APSK constellation defined by the (γ, θ) pair at E_b/N_0 given by (13) is calculated from (7) using a plot similar to Figure 7.

4. The (γ, θ) pair that maximizes $I(x; y)$ defines the optimum constellation.

We demonstrate the optimization using $\alpha = 0.5$. The symmetric information rate for (γ, θ) pairs of Figure 6 are shown in Figures 9 and 10. Figure 9 shows the three-dimensional plot of $I(x; y)$ vs. (γ, θ). The plot displays "horizontal" peaks suggesting that like the PAPR, $I(x; y)$ is more strongly dependent on γ than θ. This motivates exploring slices of $I(x; y)$ along lines of constant θ. The results are shown in Figure 10. The slice corresponding to $\theta = 0$ (the black line in Figure 10) is the maximum symmetric information rate for all values of γ. The maximum along the $\theta = 0$ curve is at $\gamma_{\text{opt}} = 2.3477$, $I_{\text{opt}}(x; y) = 3.9512$ bits/symbol, which corresponds to a code rate of $R_{\text{opt}} = 0.9878$.

The optimization procedure may be modified to account for implementation loss. The two implementation losses considered here are those for SOQPSK-TG detection and decoding for the AR4JA LDPC codes.

1. The implementation loss for SOQPSK-TG may be estimated by comparing the BER curve on page 11 of the data sheet [11] with the analytical curve for SOQPSK-TG, see for example Equation (15) of [10]. This comparison yields the SOQPSK-TG implementation loss $L_{\text{SOQPSK}} = 1$ dB.

2. The implementation loss for the length-4096 AR4JA LDPC codes [4, Appendix R] is obtained by comparing the theoretical optima of Figure 8 with the simulation results presented in Figure 7 of [12]. The curves for the length-4096 AR4JA LDPC codes in Figure 7 of [12] are about 1.5 dB to the right of theoretical bounds in Figure 8 for the $R = 1/2, 2/3, 4/5$. Assuming the same difference for the $R = 3/4$ code, we can set the implementation loss for the LDPC decoder at $L_{\text{LDPC}} = 1.5$ dB.

L_{SOQPSK} moves the operating point to the right and L_{LDPC} moves the operating point to the left. Incorporating these losses into the optimization procedure alters the operating point in step 2 as follows:

$$\left[\frac{E_b}{N_0}(\gamma,\theta)\right]_{\text{dB}} = \left[\left(\frac{E_b}{N_0}\right)^*\right]_{\text{dB}} - \left[\text{PAPR}(\gamma,\theta)\right]_{\text{dB}} + L_{\text{SOQPSK}} - L_{\text{LDPC}}. \tag{14}$$

The results corresponding to using (14) in place of (13) are shown in Figures 11 and 12. The behavior is identical to that for the ideal case with no implementation loss, except the rates are slightly lower. Figure 12 shows the slices Figure 11 along planes of constant θ. The slice corresponding to $\theta = 0$ (shown in black) produces the optimum symmetric information rate. The maximum, shown by the star, occurs at $\gamma = 2.3477$ (the same as for the unconstrained case) and is $I_{\text{opt}}(x;y) = 3.9253$ bits/symbol (or a code rate of $R_{\text{opt}} = 0.9813$).

The optimization results are summarized by the spectral efficiency plot in Figure 13. (Figure 14 is a zoomed-in view.) The spectral efficiencies for the unconstrained optimization with and without implementation losses are 2.6342 and 2.6169, respectively. The optimum points correspond to code rates of 0.9878 (no implementation loss) and 0.9813 (with implementation loss).

Also included for reference are the results corresponding to the seven DVB-S2 constellation variants. For the parameters used here, the optimum constellation and code pair identified by the optimization routine is slightly better than the best DVB-S2 option.

Because these rates do not correspond to one the AR4JA LDPC code rates in IRIG 106-15, the highest rate not greater than the unconstrained rate must be used. The spectral efficiency corresponding to these points is also plotted in the figures. But when mapped to the available AR4JA LDPC code rates, all options achieve the same spectral efficiency, but the optimum code/constellation pair has a slight link margin advantage.

Finally, the operating point for SOQPSK-TG is shown for reference. The -50 dBc bandwidth for SOQPSK-TG was used to compute its spectral efficiency. The results show that LCPC-coded 16-APSK is capable of achieving spectral efficiencies a factor of 3.95 times (unconstrained with no implementation loss), 3.93 times (unconstrained with implemented loss), and 3.20 times (AR4JA rate constrained with implementation loss) the spectral efficiency of uncoded SOQPSK-TG.

CONCLUSIONS

The 16-APSK modulation together LDPC code rates presents the system designer with a peak-to-average power ratio vs. code rate trade-off. This trade-off was recast to an optimization problem involving spectral efficiency and the constellation parameters. The optimum 16-APSK, parameterized by the (γ,θ) pair, was identified using the optimization developed in this paper. The unconstrained optimization result is 3.95 times more spectrally efficient than uncoded SOQPSK-TG. When implementation losses and the limited number of IRIG 106 LDPC code rates are factored in, the advantage drops to 3.20 times the spectral efficiency of SOQPSK-TG.

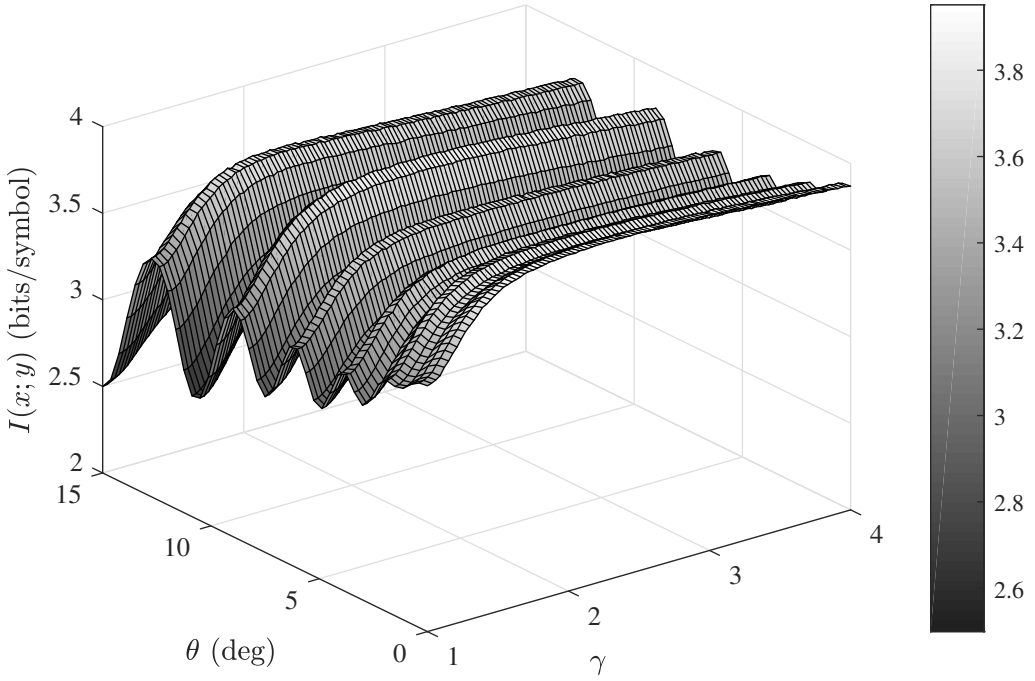

Figure 9: The symmetric information rates $I(x;y)$ corresponding to the γ, θ pairs of Figure 6.

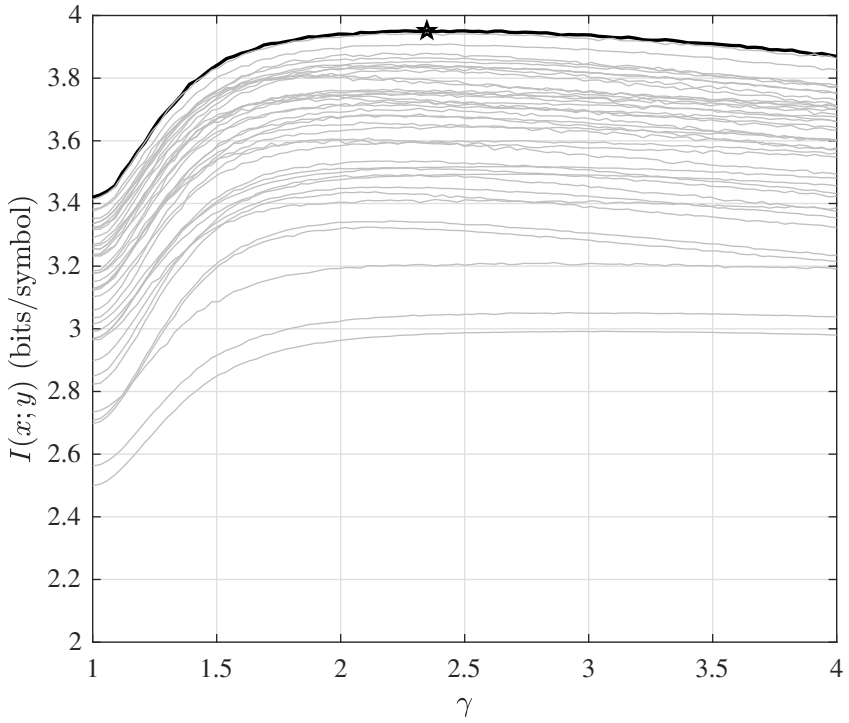

Figure 10: Slices of the three-dimensional plot of Figure 9 through constant-θ planes. The black line corresponds to $\theta = 0$. The star is placed at the maximum symmetric information rate.

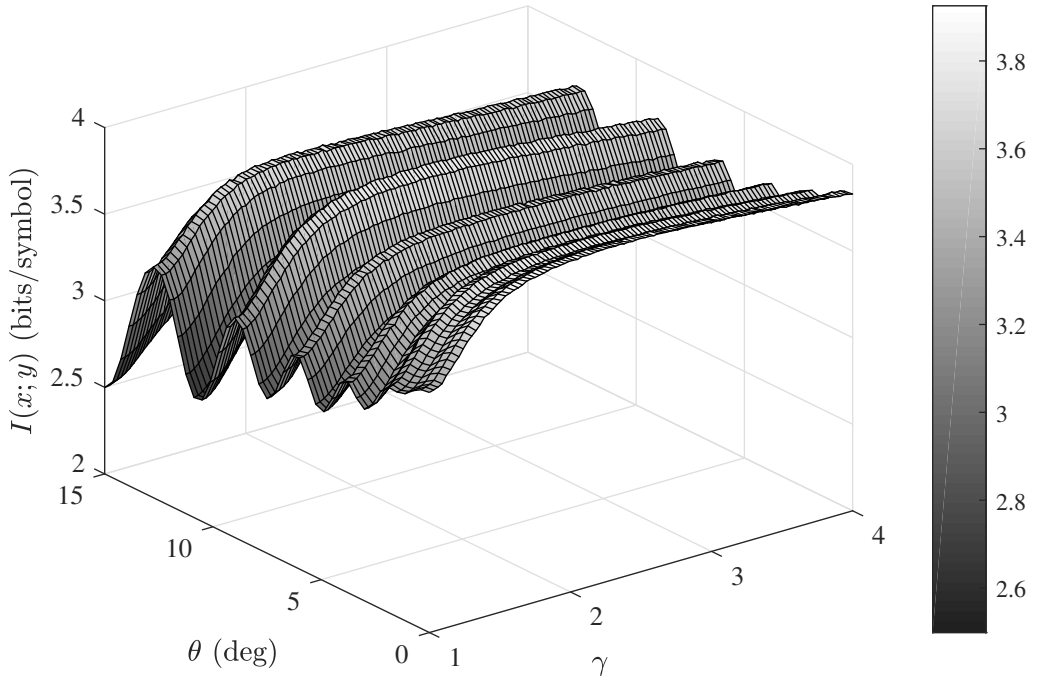

Figure 11: The symmetric information rates $I(x;y)$ corresponding to the γ, θ pairs of Figure 6 and including implementation losses $L_{\text{SOQPSK}} = 1$ dB and $L_{\text{LDPC}} = 1.5$ dB (cf. Figure 9).

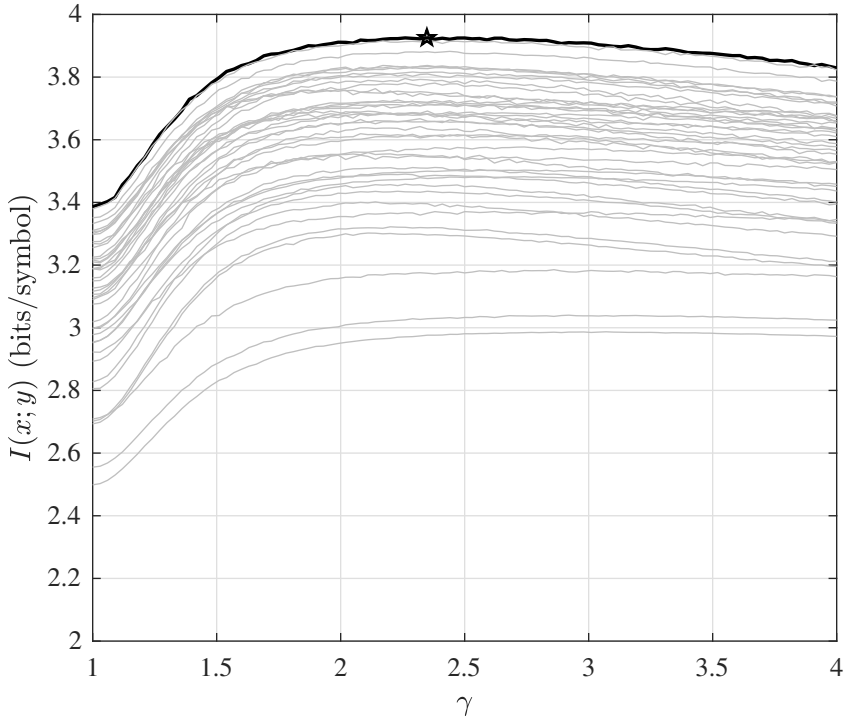

Figure 12: Slices of the three-dimensional plot of Figure 11 through constant-θ planes and including implementation losses $L_{\text{SOQPSK}} = -1$ dB and $L_{\text{LDPC}} = -1.5$ dB (cf. Figure 10). The black line corresponds to $\theta = 0$.

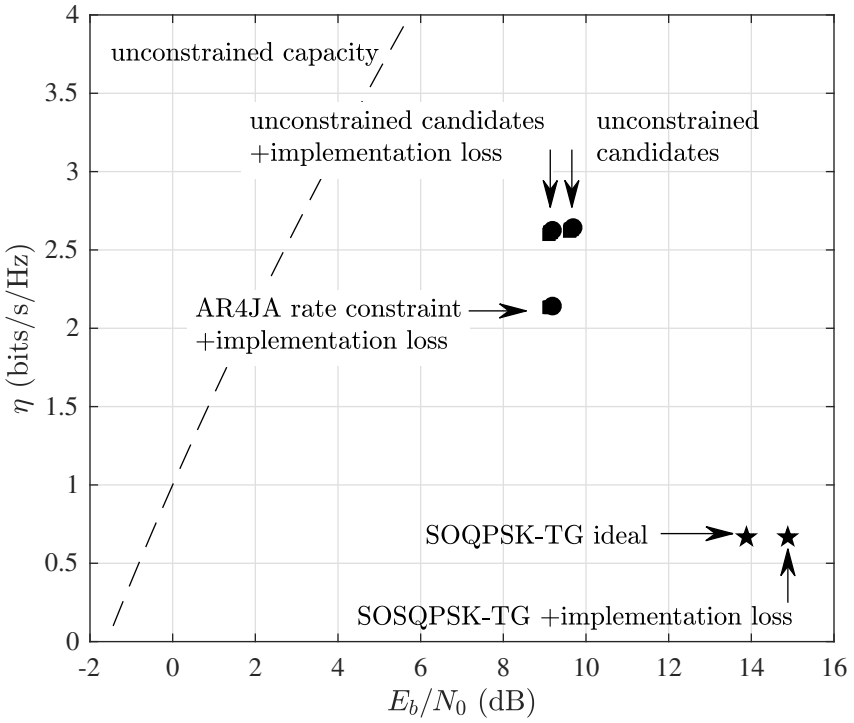

Figure 13: Spectral efficiency η SOQPSK-TG, optimum 16-APSK, and the DVB-S2 options corresponding to a target bit error probability of $P_b = 10^{-10}$ (cf. Figure 14).

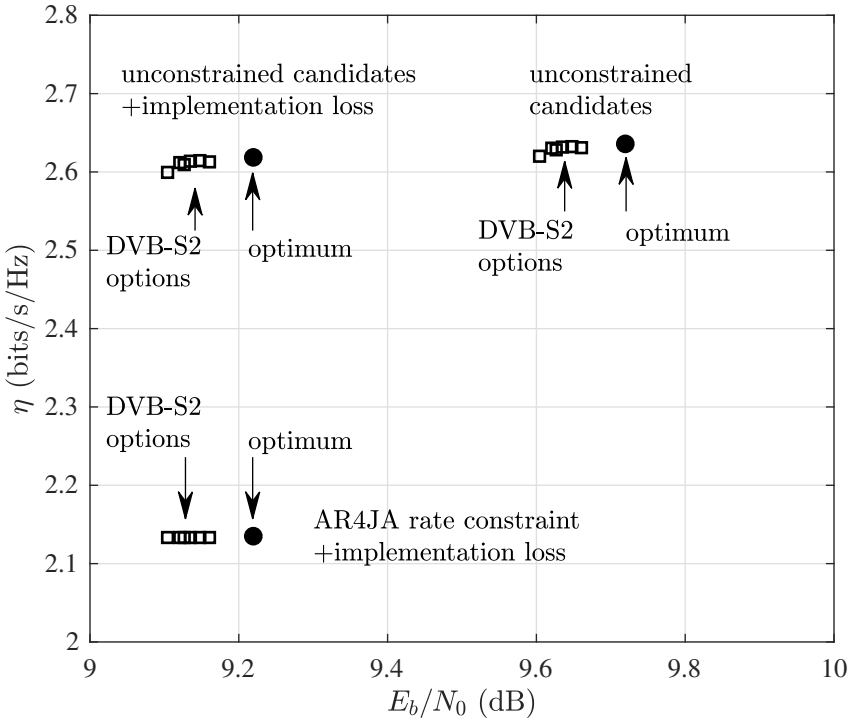

Figure 14: A close-up view of the spectral efficiency plot of Figure 13.

ACKNOWLEDGEMENTS

This project is managed by the Test Resource Management Center (TRMC) and funded through Spectrum Access R&D Program via Picatinny Arsenal under Contract No. W15QKN-15-9-1004. The Executing Agent and Program Manager work out of the AFTC.

REFERENCES

[1] Federal Communications Commission, "Auction 97: Advanced Wireless Services (AWS-3)." Available at http://wireless.fcc.gov/auctions/default.htm?job=auction_summary&id=97.

[2] ETSI EN 302 207 v1.1.2, "Digital video broadcasting (DVB): Second generation framing structure, channel coding and modulation systems for broadcasting, interactive services, new gathering and other broadband satellite applications," June 2006.

[3] C. Shaw and M. Rice, "Turbo-coded APSK for aeronautical telemetry," *IEEE Aerospace and Electronic Systems Magazine*, pp. 37–43, April 2010.

[4] Secretariat, Range Commanders Council, White Sands Missile Range, New Mexico, *IRIG Standard 106-15: Telemetry Standards*, 2015. (Available on-line at http://www.irig106.org/docs/106-15).

[5] M. Rice, *Digital Communications: A Discrete-Time Approach*. Upper Saddle River, NJ: Pearson Prentice-Hall, 2009.

[6] J. Proakis and M. Salehi, *Digital Communications*. New York, NY: McGraw-Hill, fifth ed., 2008.

[7] F. Mahmood, E. Perrins, and L. Liu, "Comprehensive energy analysis and modeling of wireless handset transceiver systems," 2017. Under review *IEEE Transactions on Green Communications and Networking*.

[8] T. Cover and J. Thomas, *Elements of Information Theory*. Hoboken, NJ: John Wiley & Sons, second ed., 2006.

[9] T. Moon, *Error Correction Coding: Mathematical Methods and Algorithms*. Hoboken, NJ: John Wiley & Sons, 2005.

[10] E. Perrins, "FEC systems for aeronautical telemetry," *IEEE Transactions on Aerospace and Electronic Systems*, vol. 49, pp. 2340–2352, October 2013.

[11] Quasonix, "3rd Generation Rack-Mount RDMS^{TM} Telemetry Receiver." Data sheet. Available at http://www.quasonix.com/sites/default/files/qsx_rackmount_thirdgen_rdms_datasheet_0.pdf.

[12] J. Hamkins, "Performance of low-density parity-check coded modulation," in *Proceedings of the IEEE Aerospace Conference*, (Big Sky, MT), 6–13 March 2010.